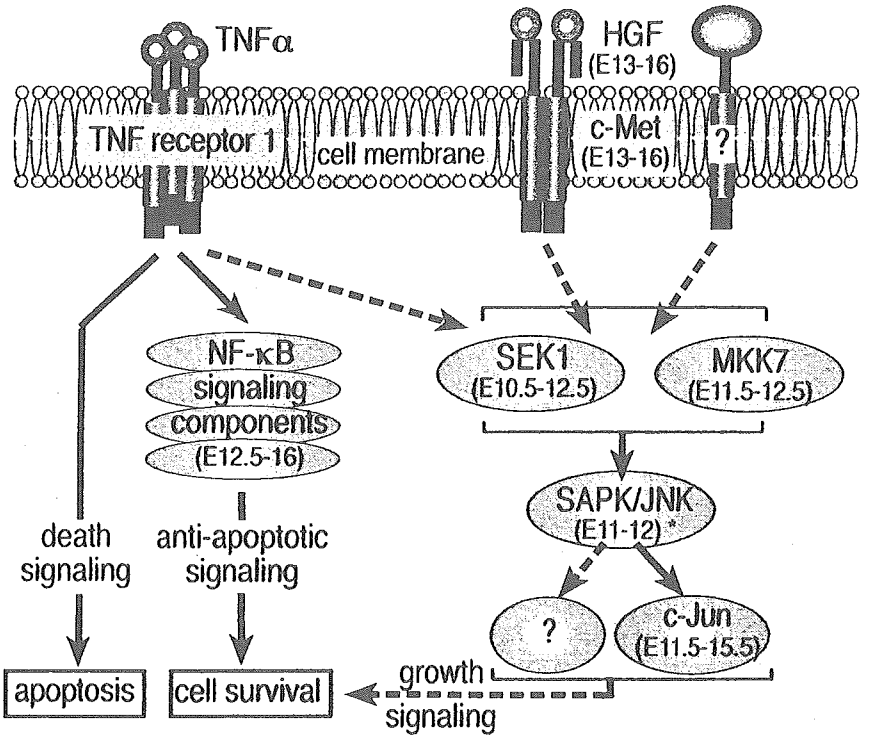

Fig. 4. Proposed model for SEK1-associated signaling pathways in hepatoblasts. The *numbers in parentheses* are days of embryonic lethality reported in previous studies and in the present study. *Solid* and *broken lines* show signaling pathways reported in previous studies and the present study, respectively. *Asterisk* indicates that *Jnk1*$^{-/-}$ *Jnk2*$^{-/-}$ mutant mice die between the eleventh and twelfth days of gestation [42] *TNF* α, tumor necrosis factor alpha, *HGF*, hepatocyte growth factor; *NF*-κB, nuclear factor kappa B; *SAPK/JNK*, stress-activated protein kinase/c-Jun N-terminal kinase

Therefore, mice lacking components of the NF-κB signaling pathway, such as RelA, IKK2, NEMO, or T2K show embryonic lethality, with massive liver apoptosis, and are rescued by the introduction of *tnfr1* mutaion. However, the physiological role of SEK1 and/or MKK7-mediated SAPK/JNK activation in response to TNFR1 stimulation remains to be resolved. In the present study, we examined the phenotype of body sizes and fetal livers of both SEK1 and TNFR1 double-knockout mice. Interestingly, embryo resorption was partially inhibited in *sek1*$^{-/-}$ *tnfr1*$^{-/-}$ mice, although the liver defect induced by *sek1* mutation was not rescued (Table 1 and Fig. 2). These results clearly show that the SEK1-mediated signal plays an important role, which is apparently different from the NF-κB signal, in fetal liver formation. Another important conclusion from the results with the *sek1*$^{-/-}$ *tnfr1*$^{-/-}$ mice is that TNFR1 plays a role in embryo resorption. Some studies have suggested the involvement of TNF-α in embryo loss and resorption by showing changes in its expression [31–33]. Our genetic experiments showing partial rescue of embryo resorption by the inactivation of TNFR1 function are consistent with the idea that TNFR1-mediated death signaling plays a role in the clearance of abnormal embryos. Thus, TNF-α elicits a wide spectrum of cellular responses, including apoptosis and cell growth. TNFR1 may relay its stimulation to SEK1-mediated cell growth in hepatoblasts, resulting in cell survival. The balance of

three separate pathways may be important for eliciting various cellular responses, depending on the type of cell and its developmental stage (Fig. 4).

To find the primary cause of the liver defect caused by *sek1* mutation, we analyzed *sek1*$^{-/-}$ livers using anti-Liv2 and found decreased numbers of hepatoblasts in the mutant embryos at E11.5. Furthermore, we found impaired BrdU incorporation into Liv2-positive hepatoblasts in *sek1*$^{-/-}$ livers at E10.5 (Fig. 3). Because liver-specific gene expression was normal in *sek1*$^{-/-}$ fetal livers, the liver defects in *sek1*$^{-/-}$ embryos are very likely due to the impaired cell growth of hepatoblasts in early hepatogenesis, resulting in decreased numbers of hepatoblasts and massive hepatoblast apoptosis. A recent report showing the maturation of SEK1-null embryonic stem cells into a hepatic lineage in vitro also indicates that the liver defect caused by *sek1* mutation is not due to impaired differentiation or maturation of hepatocytes [34]. Thus, SEK1 may provide crucial and specific growth and survival signals for hepatoblasts.

Interestingly, the findings of impaired SAPK/JNK activation in *sek1*$^{-/-}$ fetal livers extend our recent report that the synergistic activation of SAPK/JNK is impaired in SEK1-deficient murine embryonic stem cells and MKK7-deficient murine mast cells [35,36]. Furthermore, mice lacking MKK7 also show embryonic lethality between E11.5 and E12.5, with impaired liver formation and a decreased level of SAPK/JNK activation (our unpublished data). Thus, the synergistic activation of SAPK/JNK by SEK1 and MKK7 seems to occur in fetal livers and seems to be crucial for hepatoblast growth in mouse development (Fig. 4).

As described above, hepatoblast development in early hepatogenesis does not require definitive hematopoiesis. Therefore, growth factor(s), produced by nonblood cells, together with their receptor(s) on hepatoblasts, could relay SEK1 activation and promote cell growth and cell survival (Fig. 4). This idea is supported by a recent report showing that vasculogenic endothelial cells and nascent vessels are critical for the earliest stages of hepatogenesis, prior to blood-vessel function [37]. Various growth factors, such as HGF, epidermal growth factor, IL-1, and TNF-α have been implicated in hepatogenesis [38]. However, mice lacking the *TNF-α*, *TNFR1*, *IL-1*, or *IL-1R* genes did not have any defects in liver formation [39]. By contrast, HGF-deficient mice die between E13 and E16 with liver failure, and the embryonic livers are reduced in size and show extensive loss of hepatocytes [40,41]. We found that HGF is capable of stimulating SAPK/JNK activity in wild-type fetal livers at E10.5 and that the activation is markedly impaired in *sek1*$^{-/-}$ fetal livers. Thus, the HGF receptor, c-Met, is one of the candidates for relaying SEK1 activation and promoting hepatoblast growth and survival. However, *hgf*$^{-/-}$ mice die later than *sek1*$^{-/-}$ mice and have an additional defect in placental development [40,41]. Therefore, another factor(s), which could also induce SEK1 activation, may be more essential for hepatoblast growth in early hepatogenesis (Fig. 4). Thus, SEK1 may receive various signals from cell-surface receptors to regulate hepatoblast growth and survival in murine embryogenesis.

References

1. LeDouarin NM (1975) An experimental analysis of liver development. Med Biol 53: 427–455
2. Houssaint E (1980) Differentiation of the mouse hepatic primordium. I. An analysis of tissue interactions in hepatocyte differentiation. Cell Differ 9:269–279

3. Derman E, Krauter K, Walling L, Weinberger C, Ray M, Darnell JE Jr (1981) Transcriptional control in the production of liver-specific mRNAs. Cell 23:731–739
4. Panduro A, Shalaby F, Shafritz DA (1987) Changing patterns of transcriptional and post-transcriptional control of liver-specific gene expression during rat development. Genes Dev 1:1172–1182
5. Shiojiri N, Lemire JM, Fausto N (1991) Cell lineages and oval cell progenitors in rat liver development. Cancer Res 51:2611–2620
6. Tilghman SM, Belayew A (1982) Transcriptional control of the murine albumin/alpha-fetoprotein locus during development. Proc Natl Acad Sci USA 79:5254–5257
7. Watanabe T, Nakagawa K, Ohata S, Kitagawa D, Nishitai G, Seo J, Tanemura S, Shimizu N, Kishimoto H, Wada T, Aoki J, Arai H, Iwatsubo T, Mochita M, Watanabe T, Satake M, Ito Y, Matsuyama T, Mak TW, Penninger JM, Nishina H, Katada T (2002) SEK1/MKK4-mediated SAPK/JNK signaling participates in embryonic hepatoblast proliferation via a pathway different from NF-κB-induced anti-apoptosis. Dev Biol 250:332–347
8. Jung J, Zheng M, Goldfarb M, Zaret KS (1999) Initiation of mammalian liver development from endoderm by fibroblast growth factors. Science 284:1998–2003
9. Zaret KS (2000) Liver specification and early morphogenesis. Mech Dev 92:83–88
10. Kamiya A, Kinoshita T, Ito Y, Matsui T, Morikawa Y, Senba E, Nakashima K, Taga T, Yoshida K, Kishimoto T, Miyajima A (1999) Fetal liver development requires a paracrine action of oncostatin M through the gp130 signal transducer. EMBO J 18: 2127–2136
11. Davis RJ (2000) Signal transduction by the JNK group of MAP kinases. Cell 103: 239–252
12. Chang L, Karin M (2001) Mammalian MAP kinase signaling cascades. Nature 410: 37–40
13. Nishina H, Fischer KD, Radvanyi L, Shahinian A, Hakem R, Rubie EA, Bernstein A, Mak TW, Woodgett JR, Penninger JM (1997) Stress-signalling kinase Sek1 protects thymocytes from apoptosis mediated by CD95 and CD3. Nature 385:350–353
14. Nishina H, Bachmann M, Oliveira-dos-Santos AJ, Kozieradzki I, Fischer KD, Odermatt B, Wakeham A, Shahinian A, Takimoto H, Bernstein A, Mak TW, Woodgett JR, Ohashi PS, Penninger JM (1997) Impaired CD28-mediated interleukin 2 production and proliferation in stress kinase SAPK/ERK1 kinase (SEK1)/mitogen-activated protein kinase kinase4 (MKK4)-deficient T lymphocytes. J Exp Med 186:941–953
15. Nishina H, Vaz C, Billia P, Nghiem M, Sasaki T, Pompa JL, Furlonger K, Paige C, Hui CC, Fischer KD, Kishimoto H, Iwatsubo T, Katada T, Woodgett JR, Penninger JM (1999) Defective liver formation and liver cell apoptosis in mice lacking the stress signaling kinase SEK1/MKK4. Development 126:505–516
16. Yang D, Tournier C, Wysk M, Lu HT, Xu J, Davis RJ, Flavell RA (1997) Targeted disruption of the MKK4 gene causes embryonic death, inhibition of c-Jun NH2-terminal kinase activation, and defects in AP-1 transcriptional activity. Proc Natl Acad Sci USA 94:3004–3009
17. Ganiatsas S, Kwee L, Fujiwara Y, Perkins A, Ikeda T, Labow MA, Zon LI (1998) SEK1 deficiency reveals mitogen-activated protein kinase cascade crossregulation and leads to abnormal hepatogenesis. Proc Natl Acad Sci USA 95:6881–6886
18. Hilberg F, Aguzzi A, Howells N, Wagner EF (1993) c-Jun is essential for normal mouse development and hepatogenesis. Nature 365:179–181
19. Johnson RS, van Lingen B, Papaioannou VE, Spiegelman BM (1993) A null mutation at the *c-jun* locus causes embryonic lethality and retarded cell growth in culture. Genes Dev 7:1309–1317
20. Liu ZG, Hsu H, Goeddel DV, Karin M (1996) Dissection of TNF receptor 1 effector functions: JNK activation is not linked to apoptosis while NF-κB activation prevents cell death. Cell 87:565–576
21. Beg AA, Sha WC, Bronson RT, Ghosh S, Baltimore D (1995) Embryonic lethality and liver degeneration in mice lacking the RelA component of NF-κB. Nature 376:167–170

22. Li Q, Van Antwerp D, Mercurio F, Lee K-F, Verma IM (1999) Severe liver degeneration in mice lacking the IκB kinase 2 gene. Science 284:321–325
23. Li ZW, Chu W, Hu Y, Delhase M, Deerinck T, Ellisman M, Johnson R, Karin M (1999) The IKKβ subunit of IκB kinase (IKK) is essential for NF-κB activation and prevention of apoptosis. J Exp Med 189:1839–1845
24. Tanaka M, Fuentes ME, Yamaguchi K, Durnin MH, Dalrymple SA, Hardy KL, Goeddel DV (1999) Embryonic lethality, liver degeneration and impaired NF-κB activation in IKK-β-deficient mice. Immunity 10:421–429
25. Rudolph D, Yeh W-C, Wakeham A, Rudolph B, Nallainathan D, Potter J, Elia AJ, Mak TW (2000) Severe liver degeneration and lack of NF-κB activation in NEMO/IKKγ-deficient mice. Genes Dev 14:854–862
26. Bonnard M, Mirtsos C, Suzuki S, Graham K, Huang J, Ng M, Itie A, Wakeham A, Shahinian A, Henzel WJ, Elia AJ, Shillinglaw W, Mak TW, Cao Z, Yeh W-C (2000) Deficiency of T2K leads to apoptotic liver degeneration and impaired NF-κB-dependent gene transcription. EMBO J 19:4976–4985
27. Rosenfeld ME, Prichard L, Shiojiri N, Fausto N (2000) Prevention of hepatic apoptosis and embryonic lethality in RelA/TNFR-1 double knockout mice. Am J Pathol 156: 997–1007
28. Okuda T, van Deursen J, Hiebert SW, Grosveld G, Downing JR (1996) AML1, the target of multiple chromosomal translocations in human leukemia, is essential for normal fetal liver hematopoiesis. Cell 84:321–330
29. Wang Q, Stacy T, Binder M, Marin-Padilla M, Sharpe AH, Speck NA (1996) Disruption of the *Cbfa2* gene causes necrosis and hemorrhaging in the central nervous system and blocks definitive hematopoiesis. Proc Natl Acad Sci USA 93:3444–3449
30. Eferl R, Sibilia M, Hilberg F, Fuchsbichler A, Kufferath I, Guertl B, Zenz R, Wagner EF, Zatloukal K (1999) Functions of c-Jun in liver and heart development. J Cell Biol 145: 1049–1061
31. Gendron RL, Nestel FP, Lapp WS, Baines MG (1990) Lipopolysaccharide-induced fetal resorption in mice is associated with the intrauterine production of tumour necrosis factor-alpha. J Reprod Fertil 90:395–402
32. Haddad EK, Duclos AJ, Lapp WS, Baines MG (1997) Early embryo loss is associated with the prior expression of macrophage activation markers in the decidua. J Immunol 15:4886–4892
33. Lea RG, McIntyre S, Baird JD, Clark DA (1998) Tumor necrosis factor-alpha mRNA-positive cells in spontaneous resorption in rodents. Am J Reprod Immunol 39:50–57
34. Hamazaki T, Iiboshi Y, Oka M, Papst PJ, Meacham AM, Zon LI, Terada N (2001) Hepatic maturation in differentiating embryonic stem cells in vitro. FEBS Lett 497:15–19
35. Wada T, Nakagawa K, Watanabe T, Nishitai G, Seo J, Kishimoto H, Kitagawa D, Sasaki T, Penninger JM, Nishina H, Katada T (2001) Impaired synergistic-activation of stress-activated protein kinase SAPK/JNK in mouse embryonic stem cells lacking SEK1/MKK4. J Biol Chem 276:30892–30897
36. Sasaki T, Wada T, Kishimoto H, Irie-Sasaki J, Matsumoto G, Goto T, Yao Z, Wakeham A, Mak TW, Suzuki A, Katada T, Nishina H, Penninger JM (2001) The stress kinase MKK7 is a negative regulator of antigen receptor and growth factor receptor induced proliferation in hematopoietic cells. J Exp Med 194:757–768
37. Matsumoto K, Yoshitomi H, Rossant J, Zaret KS (2001) Liver organogenesis promoted by endothelial cells prior to vascular function. Science 294:559–563
38. Grisham JW, Thorgeirsson SS (1997) Liver stem cells. In: Potten CS (ed) Stem Cells. Academic, pp 233–282
39. Mittrucker HW, Pfeffer K, Schmits R, Mak TW (1996) T-lymphocyte development and function in gene-targeted mutant mice. Stem Cells 14:250–268
40. Schmidt C, Bladt F, Goedecke S, Brinkmann V, Zschiesche W, Sharpe M, Gherardi E, Birchmeire C (1995) Scatter factor/hepatocye growth factor is essential for liver development. Nature 373:699–702

41. Uehara Y, Minowa O, Mori C, Shiota K, Kuno J, Noda T, Kitamura N (1995) Placental defect and embryonic lethality in mice lacking hepatocyte growth factor/scatter factor. Nature 373:702–705
42. Kuan CY, Yang DD, Samanta Roy DR, Davis RJ, Rakic P, Flavell RA (1999) The Jnk1 and Jnk2 protein kinases are required for regional specific apoptosis during early brain development. Neuron 22:667–676

Gene Therapy (2003) 10, 406–414
© 2003 Nature Publishing Group All rights reserved 0969-7128/03 $25.00
www.nature.com/gt

RESEARCH ARTICLE

Long-term normalization in the central nervous system, ocular manifestations, and skeletal deformities by a single systemic adenovirus injection into neonatal mice with mucopolysaccharidosis VII

Y Kamata[1,2], A Tanabe[1], A Kanaji[1], M Kosuga[1,2,3], Y Fukuhara[1,3], X-K Li[1], S Suzuki[1], M Yamada[1], N Azuma[1,2] and T Okuyama[1,2,3]

[1]*National Research Institute for Child Health and Development, Tokyo, Japan;* [2]*National Center for Child Health and Development, Japan; and;* [3]*Department of Pediatrics, Keio University School of Medicine, Japan*

Systemic injection of an adenovirus vector into adult mice resulted in pathological improvements in multiple visceral organs of mice with mucopolysaccharidosis VII; however, no therapeutic efficacy was observed for mental retardation, skeletal deformities, corneal clouding, and retinal degeneration. In this study, an adenovirus vector expressing human β-glucuronidase was injected into mice with mucopolysaccharidosis VII within 24 h of birth, and therapeutic efficacy was evaluated. In the brains of the mice, more than 20% of GUSB activity was maintained for at least 20 weeks after birth, and histopathological analysis showed no obvious lysosomal storage. Furthermore, no vacuolated cells were detected in corneal stroma and retinal pigment epithelium in the eyes of the mice treated in the neonatal period, while pathological improvement was not observed in adult MPSVII mice that received similar treatments. The treated mice also lacked characteristic facial skeletal deformities, and radiographic analysis demonstrated that their facial and cranial bones were morphologically normal. These results indicate that a single systemic adenovirus injection in the neonatal period could prevent the progression of mental retardation, corneal clouding, retinal degeneration, and skeletal deformities, all of which are frequently observed clinical manifestations and difficult to treat in adulthood.
Gene Therapy (2003) **10,** 406–414. doi:10.1038/sj.gt.3301869

Keywords: *mucopolysaccharidosis; gene therapy; adenovirus; neonatal treatment*

Introduction

Mucopolysaccharidosis type VII (MPSVII, Sly disease) is a lysosomal storage disease caused by a systemic deficiency of β-glucuronidase activity.[1] This defect results in a progressive accumulation of undegraded glycosaminoglycans (GAGs) in lysosomes, and affects multiple-tissues or organs simultaneously. B6/MPSVII is a murine model of MPSVII, sharing many pathological and clinical abnormalities with human MPSVII, and both phenotypic and genotypic similarities make this animal model suitable for evaluating novel therapeutic approaches to lysosomal storage disorders.[2–4]

The therapeutic efficacy of bone marrow transplantation (BMT) and enzyme replacement therapy (ERT) for MPSVII has been investigated intensively using the murine model B6/MPSVII,[5–9] and both therapies are in clinical trials. However, certian socioeconomic and clinical problems have prevented their widespread application. Namely, a shortage of suitable donors often prevents BMT, and the cost for enzyme production and necessity of frequent injection make ERT almost impractical.

As an alternative, gene therapy for MPSVII has been explored using several viral vectors such as retroviruses,[10–12] herpes viruses,[13,14] adenoviruses,[15–20] lentiviruses,[21,22] and adeno-associated viruses.[23–26] Both *in vivo* and *ex vivo* gene transduction methods have been tested experimentally; however, only limited therapeutic success has been reported, when studies were carried out using adult B6/MPSVII. Although it is clear that a more complete pathological correction can be obtained when ERT or BMT is started from the neonatal period, the efficacy of gene therapy for neonatal MPSVII has not yet been fully investigated.

Daly *et al* recently reported widespread pathological correction of B6/MPSVII by neonatal gene transfer using an adeno-associated viral (AAV) vector.[27–28] They generated an AAV vector for expressing human β-glucuronidase under the control of the CAG promoter (a combination of the chicken β-actin promoter and cytomegalovirus enhancer), and injected it into neonatal B6/MPSVII mice. They showed persistent pathological correction in the heart, brain, retina, and liver for at least 16 weeks. However, they also found comparatively low levels of the transgene GUSB activity in all organs following adeno-associated virus-mediated gene

Correspondence: T Okuyama, National Center for Child Health and Development, 2-10-1 Okura, Setagaya-Ku, Tokyo, 157-8535, Japan
Received 22 January 2002; accepted 16 June 2002

transfer. Even at an early time point (2–3 weeks after the treatment), only heart and liver had similar levels of GUSB activity to normal B6 mice, and in the other organs (lung, kidney, brain, and spleen), very little activity (less than 10% of that in normal mice) was detected. Moreover, marked decreases in GUSB activity were observed in the serum, liver, and spleen, and activity levels in all organs except the heart were less than 10% of those in normal mice at 16 weeks after birth. Although they showed sustained therapeutic levels of GUSB (1–5% of normal GUSB levels) in multiple tissues for a year in certain mice, it may be necessary to obtain more efficient transgene expression for the treatment of human MPSVII or other lysosomal storage diseases.

We previously reported the rapid elimination of lysosomal storage in multiple visceral organs of adult B6/MPSVII mice after intravenous administration of an adenovirus-expressing human GUSB.[20] When we injected the adenoviruses into B6/MPSVII via tail veins, they were distributed predominantly in the liver, and over-produced and secreted transgene products were delivered through the systemic circulation into the lung, heart, kidney, and spleen, and subsequent amelioration of lysosomal storage was observed. However, no GUSB expression was observed in the brain, suggesting that viral infection and GUSB transport were both prevented in the brain of adult mice presumably due to blood–brain barriers.

In this study, we administered the adenovirus to newborn B6/MPSVII or normal C3H mice and transgene expression and therapeutic efficacy were observed for 20 weeks. Persistently high levels of GUSB activity were observed for the 20 weeks, and a complete amelioration of lysosomal storage occurred in all organs examined including the brain, cornea, and retina, in the tissues of which, no or little pathological correction was observed in the mice treated in adulthood. We also showed effective secondary administration of adenoviral vectors in the mice treated during the neonatal period. Furthermore, morphological correction of facial and cranial bones was achieved by the neonatal adenoviral treatment.

Results

Distribution of GUSB activity in C3H mice treated with AxCAhGUS as newborns

Human β-glucuronidase (GUSB) is heat-stable, and was reduced by only 30% after 2-h incubation at 65°C. In contrast, the GUSB of C3H mice is heat-labile, and its activity is almost completely eliminated by the same treatment.[29] Using this difference of heat stability, we evaluated the gene transduction efficiency and distribution of the transgene products by infecting normal C3H mice with adenoviral vectors. Viral solution (100 μl) containing 1×10^7 plaque-forming units (pfu) of AxCAhGUS (an adenovirus-expressing human GUSB under the control of the CAG promoter) was injected into newborn C3H mice via superficial temporal veins. The mice were sacrificed periodically, and heat-stable GUSB activity was measured in liver, spleen, kidney, lung, heart, and brain (Figure 1). Since the endogenous GUSB level of C3H mice is approximately 10–40% of the GUSB level of

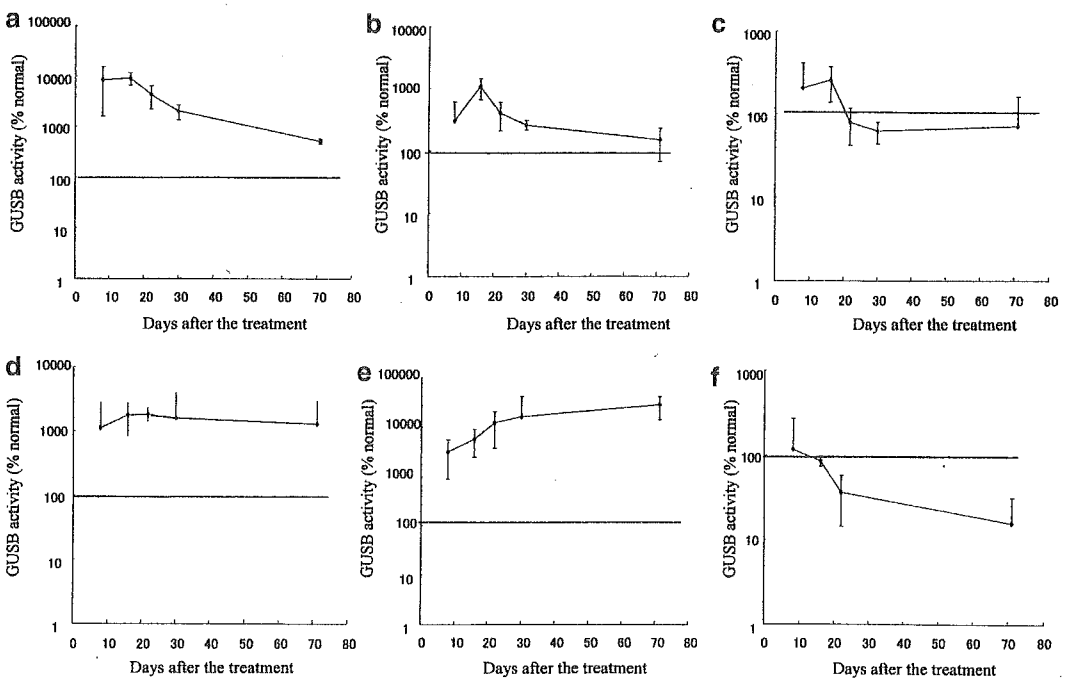

Figure 1 Time-dependent change of heat-stable β-glucuronidase (GUSB) activity in normal C3H mice infected with adenovirus-expressing human GUSB (AxCAhGUS). We injected 100 μl of viral solution containing 1×10^7 pfu of AxCAhGUS into newborn normal C3H mice within 24 h of delivery. The mice were sacrificed periodically, and heat-stable GUSB activity in each organ was measured. Each point represents the average and standard deviation for four treated animals. Results are expressed as a percentage of the GUSB activity found in the corresponding organs from four age-matched C57BL6 (B6) mice (a: liver; b: spleen; c: kidney; d: lung; e: heart; f: brain). Seven days after the treatment, high levels of the transgene activity (10–100 times higher than the GUSB activity of age-matched untreated B6 mice) were observed in liver (a), lung (d) and heart (e), while normal levels were detected in spleen (b), kidney (c) and brain (f). A time-dependent decrease of GUSB activity was observed in all examined organs, but more than 5% of the peak levels were still detected at 70 days after the treatment.

C57BL6 mice (B6 mice), we calculated '% normal activity' using GUSB level of age-matched normal B6 mice as 100%. Seven days after the treatment, high levels of the transgene (10–100 times the GUSB activity in age-matched normal B6 mice) were observed in liver, lung, and heart, while normal levels were detected in spleen, kidney, and brain (Figure 1). A time-dependent decrease of GUSB activity was observed in all examined organs, but more than 5% of the peak level was still detected even 70 days after the treatment.

Presence of viral DNA in C3H mice treated with AxCAhGUS

To determine whether the origin of the transgene GUSB in each organ is the result of transgene expression or due to cross-correction of lysosomal GUSB, viral DNA was detected with the PCR-based method (Figure 2). The PCR primers were designed based on the sequences of exons 6 and 7 of the human GUSB gene to amplify a 240-bp fragment from the human GUSB cDNA located in the viral genome of AxCAhGUS. This PCR also generates a 454-bp fragment from the endogenous murine GUSB gene.[20,30] When adult mice were infected with AxCAhGUS intravenously, a clear 240-bp DNA fragment was only detected in the PCR reaction from liver DNA, suggesting that AxCAhGUS accumulated predominantly in the liver. On the other hand, clear 240-bp DNA fragments were observed in all organs, when AxCAhGUS was intravenously administered into newborn mice, demonstrating that a significant amount of virus was distributed into multiple organs including the brain. These results indicate that the GUSB activity detected in extra-hepatic organs of the treated adult mice was due to cross-correction of a lysosomal enzyme rather than direct gene transduction; however, direct gene transduction also significantly contributed to GUSB expression in extra-hepatic organs in the mice treated as newborns.

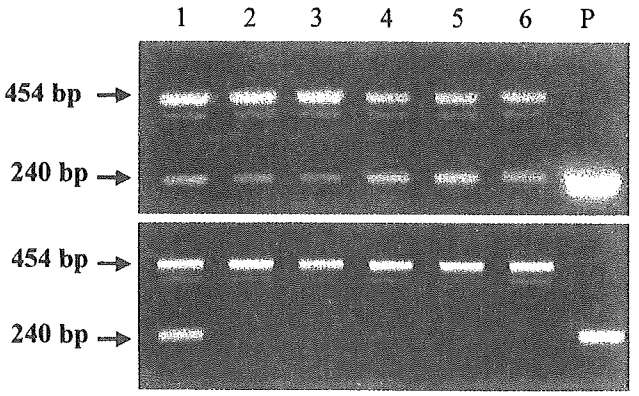

Figure 2 Detection of virally encoded human GUSB cDNA in mice treated with AxCAhGUS. We injected AxCAhGUS into C3H mice within 24 h of delivery or 30–40 days after birth. Seven days after the treatment, the mice were sacrificed and DNA from several organs was extracted and used as template for PCR. Virally encoded human GUSB cDNA in AxCAhGUS produces a 240-bp band, and the murine GUSB gene produces a 454-bp band. An intense 240-bp band was identified in all organs examined including the brain in the mice treated in the neonatal period (a), while the corresponding band was identified only in the liver in the mice treated at the age of 30–40 days. In each group, four mice were used for this experiment, and representative results are shown. Lane 1: liver; lane 2: spleen; lane 3: kidney, lane 4: lung; lane 5: heart; lane 6: brain. Lane P shows the result of the PCR reaction using human GUSB cDNA as a template.

Therapeutic efficacy of neonatal gene therapy in visceral organs

We injected an adenovirus 'AxCAhGUS' into four newborn B6/MPSVII mice and measured GUSB activity in visceral organs 30 days later. Higher than normal levels of GUSB activity (1–50 times higher than normal) were observed in liver, spleen, lung, and heart; approximately, half of the normal activity was observed in kidney (Figure 3A). Histochemical study showed disseminated GUSB-positive cells in all visceral organs, which agreed with the result of the quantification of GUSB activity (data not shown). Furthermore, histopathological analysis demonstrated complete morphological normalization in liver and spleen in the mice treated during the neonatal period (Figure 3B).

Therapeutic efficacy of neonatal gene therapy in CNS lesions

We previously showed that the intravenous administration of AxCAhGUS into adult mice resulted in significant

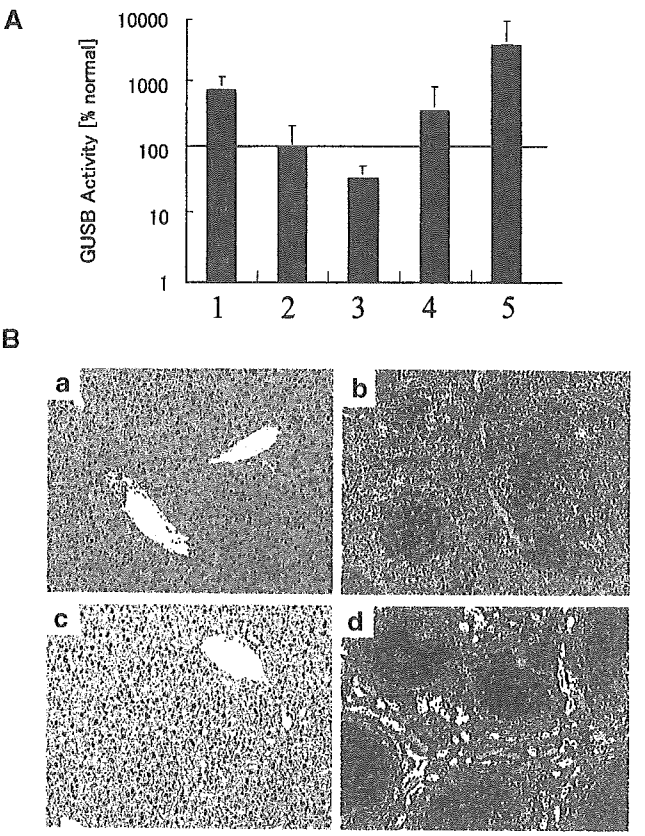

Figure 3 Therapeutic efficacy in visceral organs of B6/MPSVII mice infected with AxCAhGUS in the neonatal period. (A) We injected 100 μl of viral solution containing 1×10^7 pfu of AxCAhGUS into newborn B6/MPSVII mice within 24 h of delivery. The mice were sacrificed 30 days after the treatment and GUSB activity in each organ was measured. Each point represents the average and standard deviation for four treated animals. Results are expressed as a percentage of GUSB activity found in corresponding organs from six age-matched B6 (+/+) mice (lane 1: liver; lane 2: spleen; lane 3: kidney; lane 4: lung; lane 5: heart). (B) Histopathological study shows complete elimination of lysosome storage in liver (a) and spleen (b). For comparison, toluidine blue staining of liver (c) and spleen (d) of age-matched untreated B6/MPSVII mice is shown.

levels of GUSB expression in multiple visceral organs; however, no obvious GUSB expression was detected in the brain.[20] Since the results in C3H mice described above suggested that vector infection and subsequent GUSB expression were achievable in the mouse brain by neonatal administration, we injected AxCAhGUS into newborn B6/MPSVII mice, and therapeutic efficacy in CNS lesions was evaluated. Approximately 200% of normal GUSB activity was found in the brain 30 days after the viral injection, and 20–30% of normal GUSB activity was still detected at 140 days (Figure 4A). Histochemical study showed that disseminated GUSB-positive cells were distributed in the cortex of the mouse brain (Figure 4Ba). On the other hand, no GUSB-positive cells were detected in the brain of B6/MPSVII mice treated at 30 days after birth (Figure 4Bc). Histopathological study demonstrated that no vacuolated cells were detected even 140 days after birth (Figures 4Bd and Be).

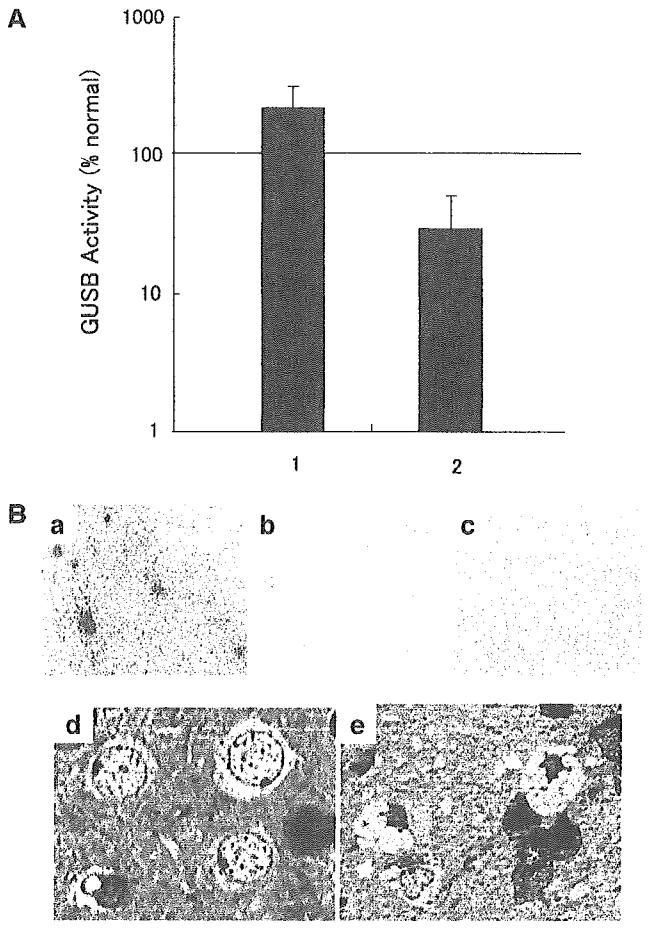

Figure 4 Therapeutic efficacy in the brains of B6/MPSVII mice infected with AxCAhGUS at neonatal period. We injected 100 μl of viral solution containing 1×10^7 pfu of AxCAhGUS into newborn B6/MPSVII mice within 24 h of delivery, and evaluated the therapeutic effect in the CNS. (A) GUSB activity in the brain of B6/MPSVII mice treated with AxCAhGUS during the neonatal period is presented. Approximately 200% and 30% of the normal level of GUSB activity was detected at 30 days (lane 1) and 140 days (lane 2) after the treatment, respectively. Each bar represents the average and standard deviation from three treated animals. Results are expressed as a percentage of GUSB activity found in the brains from four age-matched B6 (+/+) mice. (B) Histochemical study of mouse brain was performed 140 days after the neonatal treatment. Disseminated strong GUSB-positive cells are observed in the treated mice (a), while faint and diffused GUSB staining is seen in the brain of an age-matched B6 (+/+) mice (b), and no GUSB staining is seen in the brain of the B6/MPSBVII mice treated 30 days after birth (c). (C) Histopathological analysis shows no lysosomal storage in the brain cortex in the mice treated during the neonatal period (d), while characteristic vacuolation (arrows) is observed in age-matched (140 days old) untreated B6/MPSBVII mice (e).

Therapeutic efficacy of neonatal gene therapy against ocular complications

Retinal degeneration and corneal clouding are frequently observed as ocular complications in MPSVII or other mucopolysaccharidoses.[31,32] We studied the therapeutic efficacy in the retina and cornea of B6/MPSVII mice treated by systemic vector administration in the neonatal period. In the retina of the mice treated in adulthood, no or few GUSB-positive cells were identified among the retinal pigment epithelial cells where lysosomal storage is remarkable in the affected mice (Figures 5Aa and Ac). In contrast, these cells were clearly GUSB-positive in the mice treated in the neonatal period, and subsequent improvement of lysosomal storage was observed (Figures 5Ab and Ad). In the cornea, histochemical study indicated that disseminated GUSB-positive cells were present in the stroma, and subsequent amelioration of lysosomal storage was observed (Figures 5Bb and Bd) in the mice treated during the neonatal period. However, no obvious pathological correction was observed in the cornea of the mice treated in adulthood (Figures 5Ba and Bc). These results show that effective therapeutic results for ocular complications by systemic administration can be obtained only when the injection is carried out in the neonatal period.

Improvement of skeletal deformities by neonatal treatment

Skeletal deformity is another frequent and serious manifestation in patients suffering from all types of mucopolysaccharidoses. A flattened face is a characteristic phenotype of skeletal deformity in B6/MPSVII. All the mice that received neonatal treatment were of normal facial appearance even at 140 days after the treatment, and radiographic analysis showed morphological normalization of facial and cranial bones in the mice treated in the neonatal period (Figure 6). On the other hand, no obvious improvement in skeletal deformities was observed on adenovirus treatment in adult mice (data not shown), suggesting that neonatal or infantile gene therapy is essential for preventing skeletal deformities in MPSVII.

Feasibility of gene transduction by multiple vector administrations

The feasibility of gene transduction by multiple vector administrations was studied by quantification of serum GUSB activity in the MPSVII mice treated in the neonatal period. About 5–10 times higher than normal GUSB activity was observed 35 days after the treatment (Figure 7). Since no increase in the titers of anti-adenoviral neutralizing antibody was observed in the same serum samples (Table 1), we attempted a secondary viral administration at 35 days after birth. A rapid and marked increase of serum GUSB activity was identified 7 days after the secondary injection, and this high level of the activity was maintained for more than 100 days after birth (Figure 7). However, the mice generated significant

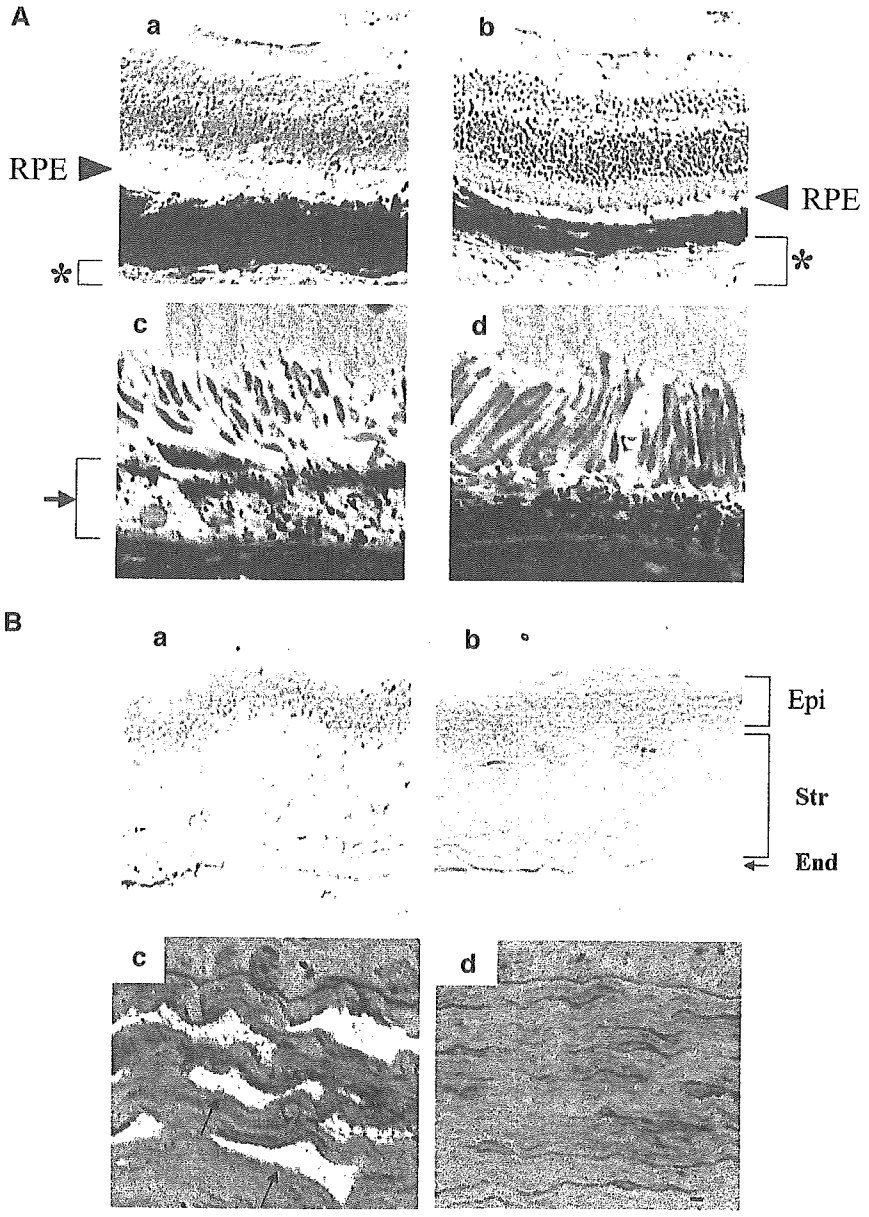

Figure 5 Therapeutic efficacy for ocular manifestations in B6/MPSVII mice infected with AxCAhGUS in the neonatal period. Newborn and adult B6/MPSVII mice were infected with AxCAhGUS, their eyes were enucleated 140 or 7 days after the treatment, respectively, and therapeutic efficacy in the retina (A) and cornea (B) was evaluated. (A) In the mice that received neonatal treatment (Ab), GUSB-positive cells are identified among retinal pigment epithelial cells (RPE) as well as in tissues outside of retina (asterisk), while in the mice treated in adulthood (Aa), GUSB-positive cells are only located in tissues outside of retina. Histopathological study shows amelioration of lysosomal storage in the mice treated during the neonatal period (Ad), but no pathological correction in the mice treated in adulthood (Ac). An arrow indicates vacuolated RPE cells due to lysosomal storage. (B) In corneal tissues, GUSB-positive cells are distributed in the corneal stroma (Str) only in the mice treated in the neonatal period (Bb), and no GUSB-positive cells are detected in adulthood (Ba). Elimination of lysosomal storage is observed in the mice that received neonatal treatment (Bd), but no correction is seen in the mice that treated in adulthood (Bc). Arrows indicate characteristic vacuolization due to lysosomal storage. Epi: epithelium; Str: stroma; End: endothelium.

levels of anti-adenoviral neutralizing antibody (32–128 titers) 2 months after the secondary injection (Table 1). Moreover, no increase of serum GUSB activity was observed 7 days after tertiary vector administration (Figure 7).

Discussion

We previously reported the therapeutic efficacy of adenovirus-mediated gene therapy in adult MPSVII mice.[20] In the report, we demonstrated that high levels of GUSB activity in multiple extrahepatic organs such as spleen, kidney, lung, and heart were the result of *in vivo* cross-correction of GUSB delivered from the liver, where gene transduction had taken place. A rapid and complete amelioration of lysosomal storage was also observed in liver and spleen in the treated animals. These experiments, however, also disclosed the limitations of this treatment strategy. First, no significant GUSB activity was identified in the brain, which is one of the most important affected regions in MPSVII as well as other

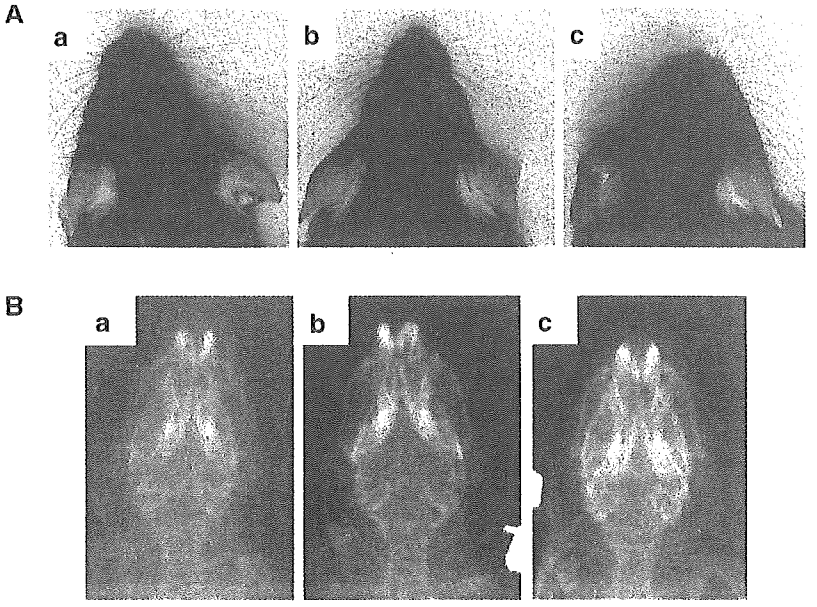

Figure 6 Therapeutic efficacy for skeletal deformity in B6/MPSVII. A flattened face is a characteristic symptom of skeletal deformity in B6/MPSVII. The faces of the mice (140 days old) that received neonatal adenoviral injection (Ab) are indistinguishable from those of the B6 (+/+) littermates (Aa), while an untreated MPSVII littermate show characteristic deformity (Ac). Radiographic analysis also indicates a remarkable improvement of facial and cranial bone deformities in the treated animal (Ba: normal littermate, Bb: a treated animal, Bc: untreated B6/MPSVII littermate).

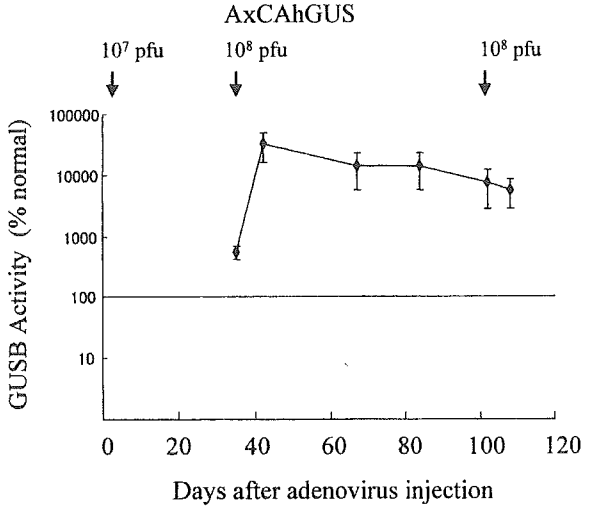

Figure 7 Time-dependent change of serum GUSB activity in the mice treated with AxCAhGUS. To investigate the feasibility of gene transduction by multiple vector injections, we performed periodic serum sampling from the mice infected with AxCAhGUS during the neonatal period. A 10-fold higher than normal GUSB activity was still identified in the mice 5 weeks after the treatment. Secondary vector administration was carried out just after the serum sampling. A week later, serum GUSB activities were measured again. A marked increase in serum GUSB activity was observed, and this high level of activity was maintained for more than 60 days. However, no obvious increase in GUSB activity was observed when a tertiary administration was performed 120 days after the first administration. Each point represents the mean and standard deviation from four treated animals. Results are expressed as a percentage of the GUSB activity in four age-matched B6 (+/+) mice. Arrows indicate the day when the vector injection was done. For the first administration, 100 μl of the vector solution containing 1×10^7 pfu of AxCAhGUS was injected into neonatal B6/MPSVII mice via superficial temporal veins. For secondary and tertiary administration, 1 ml of vector solution containing 1×10^8 pfu of AxCAhGUS was injected into B6/MPSVII mice via tail veins.

lysosomal storage disorders. Second, no pathological correction was observed in retina and cornea. Third, no improvement of skeletal deformities was found. Finally, the therapeutic effect did not persist for long.

Mental retardation is a frequent manifestation in several types of mucopolysaccharidoses as well as other lysosomal storage disorders.[33] We and other groups achieved successful pathological correction in the CNS by transplantation of GUSB-producing cells,[11,18] or by generation of GUSB-producing cells in the brain with direct vector administrations.[16] Although these therapeutic strategies may be effective, less invasive approach is required for widespread clinical applications. Sands *et al* showed that for BMT or ERT, it is necessary to start the treatments in the neonatal period to prevent degenerations of the CNS.[5,7,9] Daly *et al* have recently shown that neonatal gene transfer is also effective for treating the CNS in MPSVII using adeno-associated virus vectors.[27] They showed that the GUSB activity in the brain after AAV-mediated gene transduction was less than 10% of the activity in normal littermates. Although 1–5% of normal activity may be sufficient for the treatment in this particular disease model, a comparatively inefficient gene transduction may cause the problem in the treatment of human MPSVII or other lysosomal storage diseases. In the present study, we demonstrated that 20–30% of normal GUSB activity was detected in the mouse brain even 140 days after the adenovirus treatment. These observations indicate that an adenoviral gene transfer seems to be more efficient than the treatment with AAV vectors, although physiological and behavioral studies will have to be performed to prove this.

The blood–brain barrier is the main reason why both vector infection and GUSB transport were prevented in adult mouse brain.[34] The blood–retinal barrier is also a

hurdle in the delivery of drug to the cells in the retina from the systemic circulation.[35] In this paper, we have reported that no GUSB-positive cells were detected among retinal pigment epithelial cells, and lysosomal storage was not eliminated in the adult mice treated by adenovirus vectors. This finding suggests that the blood–retinal barrier prevented both vector infection and uptake of GUSB into the retinal pigment epithelial cells. On the other hand, long-term GUSB expression and pathological correction were observed in the mice treated in the neonatal period. Although it is unclear whether the blood–retinal barrier is immature in neonatal mice just like the blood–brain barrier, immaturity of the barriers may have enabled the vector infection to occur in retinal cells.[34]

Here, we also showed that lysosomal storage in corneal stroma was completely eliminated in the mice treated during the neonatal period, while no obvious efficacy was seen in the mice treated in adulthood. This finding is unexpected but favorable in terms of treatment of corneal clouding, which is the most frequent ocular manifestation in several types of mucopolysaccharidoses.[33]

We also showed improvement of skeletal deformities following neonatal treatment. In the mice treated after maturation, no obvious improvement of facial dysmorphology was achieved. However, the facial appearance of the mice treated in the neonatal period was completely normal. Radiographic analysis showed that their facial and cranial bones were also morphologically normal. These results demonstrate that a single vector injection during the neonatal period is sufficient for complete normalization of the facial and cranial bones in MPSVII.

One of the most important findings in this study is the remarkable difference in vector targeting organs after intravenous injection between neonatal and adult treatment. As we showed previously, most of the vectors were accumulated in the liver when we injected virus in adult mice.[20] On the other hand, the vectors were distributed in all organs examined when injection was carried out in the neonatal period. Fechner *et al* reported that anatomic vector barriers, in particular the endothelium structure, were the major factors in determining the vector-targeting organs, and the expression of viral receptors did not correlate with adenoviral vector targeting.[36] This suggests that immaturity of the blood–brain barrier and blood–retinal barrier is a major factor for determining vector-targeting organs, although the difference of the site of injection between newborn MPSVII and adult MPSVII might also partially account for the difference of the vector-targeted organs.

Since an exogenously transduced gene delivered by adenoviral vectors is episomal, dilution of the transgene should take place with the growth of the vector-infected organs or tissues. This indicates the necessity for multiple vector administrations to obtain long-term therapeutic efficacy especially for neonatal treatment. In this report, we demonstrated the feasibility of secondary gene transduction in mice treated initially during the neonatal period. However, anti-adenovirus antibody was generated after secondary treatment, and tertiary injection did not induce efficient gene transduction. These observations suggest that neonatal mice can avoid the deleterious immune response induced by infection with adenovirus vectors. Reducing the immune response that accompanies adenoviral vector infection is essential not only to prolong the transgene expression but also to carry out adenovirus-mediated gene therapy safely.

Here we showed that a single adenoviral infection in the neonatal period is sufficient to prevent the progression of multiple tissue lesions in the CNS, ocular tissues and skeletal system in MPSVII mice. Since humans are rather more developed at birth than mice in terms of the blood–brain barrier, we may have to consider fetal gene therapy (*in utero* gene therapy) to achieve the similar therpeutic efficacy in human MPSVII. The molecular genetics of lysosomal storage diseases has been intensively investigated, and prenatal diagnosis of lysosomal storage diseases is now available. Although several safety issues have to be resolved before clinical applications, neonatal or fetal treatment with an adenoviral vector combined with prenatal diagnosis is a promising strategy for MPSVII and other lysosomal storage disorders.

Table 1 Serum anti-adenovirus titers of the mice treated with AxCAhGUS

	Titers of serum anti-adenovirus
1 month after neonatal treatment	<2 (n=7)
2 months after secondary treatment	32, 32, 64, 128
1 month after the treatment in adult mice	128, 256, 256

Materials and methods

Adenoviruses

The two adenoviruses, AxCAhGUS and AxCALacZ, used in this study were E1/E3-deleted recombinant adenoviruses expressing human β-glucuronidase (GUSB) and *E. coli* β-galactosidase (lacZ), respectively.[19,20] Both viruses were generated based on the COS-TPC method described previously.[37] Briefly, a cosmid, pAxCAhGUS, which contained an expression cassette of human GUSB under the control of the CAG promoter,[38] was constructed by subcloning cDNA for human GUSB at a unique *Swa*I site of pAxCAwt. Then 293 cells were co-transfected with the cosmid pAxCAhGUS and an adenoviral DNA–terminal protein complex, which had already been digested at several sites with *Eco*T22I. A recombinant adenovirus was generated through homologous recombination in the transfected cells. Another adenoviral vector AxCALacZ was supplied by Dr I Saito.[39]

Animals

Syngeneic B6/MPSVII mice were obtained from a pedigree colony of B6.C-H-2bml/ByBir-gusmps/+ mice maintained at the National Children's Medical Research Center.[2,3] Normal C3H mice were purchased from Shizuoka Laboratory Animal Center (Shizuoka, Japan). All mice were maintained in accordance with the guidelines of the animal committee of the facility.

Neonatal injections

Viral solution (100 μl) containing 1×10^7 pfu of AxCAhGUS was injected into newborn B6/MPSVII mice (n=8)

or normal C3H mice (n=30) via the superficial temporal veins within 24 h of delivery.[27,28] For comparison, adult B6 (+/+) mice (n=12) were injected with 1 ml of viral solution containing 1×10^8 pfu of AxCAhGUS via tail veins.

Detection of viral DNA in mouse organs

The total DNA of tissue samples was extracted using a QIAamp DNA mini kit (Qiagen GmbH, Hilden, Germany) according to the manufacturer's protocol. Viral DNA in each tissue was detected using PCR to amplify the partial cDNA for human GUSB based on a method described previously.[20] Briefly, the forward and reverse primers were synthesized from the sequence of exons 6 and 7. Expected products are 240-bp fragments from human cDNA encoded in the viral genome of AxCAhGUS. Since these primer sequences were identical to the corresponding regions of the murine GUSB gene with two mismatches, 454-bp DNA fragments were amplified when PCR was carried out using mouse genomic DNA as template.

Quantitative and histochemical analysis of GUSB activity

GUSB activity in tissue was quantified using a fluorometric assay described previously.[40] Briefly, tissues were homogenized in 10 mM Tris–HCl (pH 7.5), 150 mM NaCl, 0.2% Triton X-100, and 1 mM dithiothreitol. When necessary, the samples were incubated for 2h at 65°C to inactivate endogenous GUSB in normal C3H mice. GUSB activity was measured using 4-methylumbelliferyl β-D-glucuronide (Sigma, St. Louis, MO, USA) as substrate. Histochemical detection of GUSB activity was performed on 6-μm-thick frozen sections using naphtol AS-BI β-D-glucuronide (Sigma) as substrate. Tissues were then counterstained with methyl green (Muto Chemistry, Tokyo, Japan).

Histopathological analysis of lysosomal storage

Tissues were isolated from the mice, and immediately immersed in cold 2% glutaraldehyde in 0.1 M. cacodylate buffer, postfixed in 1% osmium tetroxide, dehydrated through a graded series of ethanol solutions, and embedded in Spurr's Medium (Polyscience, Warrington, PA, USA). Three micrometers thick frozen section were stained with toluidine blue for evaluation of lysosomal storage. Histological sections were evaluated morphologically by light microscopy.[18]

Anti-adenoviral neutralizing antibodies

Anti-adenovirus neutralizing antibodies in serum were measured as described previously with minor modifications.[41] Briefly, the serum samples were heat-inactivated at 55°C for 30 min and diluted in the medium in two steps. Each serum dilution (0.1 ml) was mixed with 5×10^5 pfu of AxCALacZ (10 μl), incubated at 37°C for 90 min, and applied to nearly confluent 293 cells in a 96-well plate for 10 h. The supernatant, containing serum and viruses, was then replaced with normal medium for 18h. Cells were fixed and stained with X-gal. In the absence of neutralizing antibody, all of the cells stained blue. Titers of the neutralizing antibody for each serum sample were reported as the highest dilution at which less than 25% of the cells stained blue.

Acknowledgements

We thank Drs Y Kanegae and I Saito for recombinant adenovirus constructs and Dr J Miyazaki for the CAG promoters. This work was supported in part by grants for Pediatric Research from the Ministry of Health, Labor, and Welfare, Japan, and by grants for Research on Health Sciences focusing on Drug Innovation from the Japan Health Sciences Foundation.

References

1 Sly WS, Quinton BA, McAlister WH, Rimoin DL. β-glucuronidase deficiency: report of clinical, radiologic, and biochemical features of a new mucopolysaccharidosis. *J Pediatr* 1973; **82**: 249–257.
2 Birkenmeier EH *et al*. Murine mucopolysaccharidosis type VII. Characterization of a mouse with beta-glucuronidase deficiency. *J Clin Invest* 1989; **83**: 1258–1266.
3 Sands MS, Birkenmeier EH A single-base-pair deletion in the beta-glucuronidase gene accounts for the phenotype of murine mucopolysaccharidosis type VII. *Proc Natl Acad Sci USA* 1993; **90**: 6567–6571.
4 Sands MS *et al*. Gene therapy for murine mucopolysaccharidosis type VII. *Neuromuscul Disord* 1997; **7**: 352–360.
5 Sands MS *et al*. Enzyme replacement therapy for murine mucopolysaccharidosis type VII. *Clin Invest* 1994; **93**: 2324–2331.
6 Vogler C *et al*. Murine mucopolysaccharidosis type VII: long term therapeutic effects of enzyme replacement and enzyme replacement followed by bone marrow transplantation. *J Clin Invest* 1997; **99**: 1596–1605.
7 Vogler C *et al*. Enzyme replacement in murine mucopolysaccharidosis type VII: neuronal and glial response to β-glucuronidase requires early initiation of enzyme replacement therapy. *Pediatr Res* 1999; **45**: 838–844.
8 Sands MS *et al*. Syngeneic bone marrow transplantation reduces the hearing loss associated with murine mucopolysaccharidosis type VII. *Blood* 1995; **86**: 2033–2040.
9 Sands MS *et al*. Treatment of murine mucopolysaccharidosis type VII by syngeneic bone marrow transplantation in neonates. *Lab Invest* 1993; **68**: 676–686.
10 Wolfe JH *et al*. Reversal of pathology in murine mucopolysaccharidosis type VII by somatic cell gene transfer. *Nature* 1992; **360**: 749–753.
11 Taylor RM, Wolfe JH. Decreased lysosomal storage in the adult MPS VII mouse brain in the vicinity of grafts of retroviral vector-corrected fibroblasts secreting high levels of beta-glucuronidase. *Nat Med* 1997; **3**: 771–774.
12 Taylor RM, Wolfe JH. Cross-correction of β-glucuronidase deficiency by retroviral vector-mediated gene transfer. *Exp Cell Res* 1994; **214**: 606–613.
13 Zhu J, Kang W, Wolfe JH, Fraser NW. Significantly increased expression of β-glucuronidase in the central nervous system of mucopolysaccharidosis type VII mice from the latency-associated transcript promoter in a nonpathogenic herpes simplex virus type 1 vector. *Mol Ther* 2000; **2**: 82–94.
14 Wolfe JH, Deshmane SL, Fraser NW. Herpesvirus vector gene transfer and expression of beta-glucuronidase in the central nervous system of MPS VII mice. *Nat Genet* 1992; **1**: 379–384.
15 Ghodsi A *et al*. Systemic hyperosmolality improves β-glucuronidase distribution and pathology in murine MPS VII brain following intraventricular gene transfer. *Exp Neurol* 1999; **160**: 109–116.
16 Ghodsi A *et al*. Extensive β-glucuronidase activity in murine central nervous system after adenovirus-mediated gene transfer to brain. *Hum Gene Ther* 1998; **9**: 2331–2340.

17 Ohashi T *et al.* Adenovirus-mediated gene transfer and expression of human β-glucuronidase gene in the liver, spleen, and central nervous system in mucopolysaccharidosis type VII mice. *Proc Natl Acad Sci USA* 1997; **94**: 1287–1292.
18 Kosuga M *et al.* Engraftment of genetically engineered amniotic epithelial cells corrects lysosomal storage in multiple areas of the brain in mucopolysaccharidosis type VII mice. *Mol Ther* 2001; **3**: 139–148.
19 Kosuga M *et al.* Phenotype correction in murine mucopolysaccharidosis type VII by transplantation of human amniotic epithelial cells after adenovirus-mediated gene transfer. *Cell Transplant* 2000; **9**: 687–692.
20 Kosuga M *et al.* Adenovirus-mediated gene therapy for mucopolysaccharidosis VII: involvement of cross-correction in wide-spread distribution of the gene products and long-term effects of CTLA-4Ig coexpression. *Mol Ther* 2000; **1**: 406–413.
21 Stein CS *et al. In vivo* treatment of hemophilia A and mucopolysaccharidosis type VII using nonprimate lentiviral vectors. *Mol Ther* 2001; **3**: 850–856.
22 Bosch A *et al.* Reversal of pathology in the entire brain of mucopolysaccharidosis type VII mice after lentivirus-mediated gene transfer. *Hum Gene Ther* 2000; **11**: 1139–1150.
23 Sferra TJ *et al.* Recombinant adeno-associated virus-mediated correction of lysosomal storage within the central nervous system of the adult mucopolysaccharidosis type VII mouse. *Hum Gene Ther* 2000; **11**: 507–519.
24 Daly TM *et al.* Neonatal intramuscular injection with recombinant adeno-associated virus results in prolonged β-glucuronidase expression *in situ* and correction of liver pathology in mucopolysaccharidosis type VII mice. *Hum Gene Ther* 1999; **10**: 85–94.
25 Skorupa JH *et al.* Sustained production of β-glucuronidase from localized sites after AAV vector gene transfer results in widespread distribution of enzyme and reversal of lysosomal storage lesions in a large volume of brain in mucopolysaccharidosis VII mice. *Exp Neurol* 1999; **160**: 17–27.
26 Elliger SS *et al.* Elimination of lysosomal storage in brains of MPS VII mice treated by intrathecal administration of an adeno-associated virus vector. *Gene Ther* 1999; **6**: 1175–1178.
27 Daly TM *et al.* Neonatal gene transfer leads to widespread correction of pathology in a murine model of lysosomal storage disease. *Proc Natl Acad Sci USA* 1999; **96**: 2296–2300.
28 Daly TM *et al.* Prevention of systemic clinical disease in MPS VII mice following AAV-mediated neonatal gene transfer. *Gene Ther* 2001; **8**: 1291–1298.
29 Wu BM *et al.* Overexpression rescues the mutant phenotype of L176F mutation causing beta-glucuronidase deficiency mucopolysaccharidosis in two Mennonite siblings. *J Biol Chem* 1994; **269**: 23681–23688.
30 Oshima A *et al.* Cloning, sequencing, and expression of cDNA for human β-glucuronidase. *Proc Natl Acad Sci USA* 1987; **84**: 685–689.
31 Chijiiwa T, Inomata H, Yamana Y, Kaibara N. Ocular manifestations of Hurler/Scheie phenotype in two sibs. *Jpn J Ophthalmol* 1983; **27**: 54–62.
32 Mollard RJ, Telegan P, Haskins M, Aguirre G. Corneal endothelium in mucopolysaccharide storage disorders. Morphologic studies in animal models. *Cornea* 1996; **15**: 25–34.
33 Neufeld EF, Muenzer J. The mucopolysaccharidoses. In: Scriver C, Beudet A, Sly W, Valle D (eds). *The Metabolic and Molecular Basis of Inherited Diseases*. McGraw-Hill: New York, 1995, pp. 2465–2494.
34 Stewart PA, Hayakawa EM. Interendothelial junctional changes underlie the developmental 'tightening' of the blood–brain barrier. *Brain Res* 1987; **429**: 271–281.
35 Cunha-Vaz JG. The blood–ocular barriers: past, present, and future. *Doc Ophthalmol* 1997; **93**: 149–157.
36 Fechner H *et al.* Expression of coxsackie adenovirus receptor and alphav-integrin does not correlate with adenovector targeting *in vivo* indicating anatomical vector barriers. *Gene Ther* 1999; **6**: 1520–1535.
37 Miyake S *et al.* Efficient generation of recombinant adenoviruses using adenovirus DNA-terminal protein complex and a cosmid bearing the full-length virus genome. *Proc Natl Acad Sci USA* 1996; **93**: 1320–1324.
38 Miyazaki J *et al.* Expression vector system based on the chicken beta-actin promoter directs efficient production of interleukin-5. *Gene* 1989; **79**: 269–277.
39 Kanegae Y *et al.* Efficient gene activation in mammalian cells by using recombinant adenovirus expressing site-specific Cre recombinase. *Nucleic Acids Res* 1995; **23**: 3816–3821.
40 Wholfe JH, Sands MS. Murine mucopolysaccharidosis type VII: a model system for somatic gene therapy of the central nervous system. In: Lowenstein P, Enquist L (eds). *Gene Transfer into Neurons towards Gene Therapy of Neurological Disorders*. Wiley: Essex, UK, 1996; pp. 263–274.
41 Ilan Y *et al.* Transient immunosuppression with FK506 permits long-term expression of therapeutic genes introduced into the liver using recombinant adenoviruses in the rat. *Hepatology* 1997; **26**: 949–956.

Am. J. Hum. Genet. 72:1565–1570, 2003

Report

Mutations of the *PAX6* Gene Detected in Patients with a Variety of Optic-Nerve Malformations

Noriyuki Azuma,[1,2] Yuki Yamaguchi,[3] Hiroshi Handa,[3] Keiko Tadokoro,[2] Atsuko Asaka,[2] Eriko Kawase,[1,2] and Masao Yamada[2]

[1]Department of Ophthalmology, National Center for Child Health and Development, and [2]Department of Genetics, National Research Institute for Child Health and Development, Tokyo; and [3]Department of Biomolecular Engineering, Frontier Collaborative Research Center, Tokyo Institute of Technology, Yokohama, Japan

The *PAX6* gene is involved in ocular morphogenesis and is expressed in the developing central nervous system and numerous ocular tissues during development. *PAX6* mutations have been detected in various ocular anomalies, including aniridia, Peters anomaly, corneal dystrophy, congenital cataracts, and foveal hypoplasia. However, it has not been identified in patients with optic-nerve malformations. Here, we identified novel mutations in eight pedigrees with optic-nerve malformations, including coloboma, morning glory disc anomaly, optic-nerve hypoplasia/aplasia, and persistent hyperplastic primary vitreous. A functional assay demonstrated that each mutation decreased the transcriptional activation potential of PAX6 through the paired DNA-binding domain. PAX6 and PAX2 are each thought to downregulate the expression of the other. Four of the detected mutations affected PAX6-mediated transcriptional repression of the *PAX2* promoter in a reporter assay. Because *PAX2* gene mutations were detected in papillorenal syndrome, alternation of PAX2 function by *PAX6* mutations may affect phenotypic manifestations of optic-nerve malformations.

Previous ophthalmoscopy and medical imaging studies have established a variety of clinical entities in optic-nerve malformation (Brown and Tasman 1983), since numerous tissues and developmental events contribute to the optic-nerve architecture. The optic nerve first arises as the optic stalk between the forebrain and optic vesicle at 3 wk human gestation. At 5–6 wk, mesenchymes and vessels invade through the embryonic fissure, a transiently appearing ventral cleft of the optic stalk and optic cup, into the vitreous cavity. Nerve fibers of retinal ganglion cells then begin to project into the CNS at 8–10 wk. In the middle stage, the optic nerve is coated with a collagen sheath and propped up by glial cells, and the nerve head is transiently covered with glial cells and hyaloid vessels. In this series of events, developmental failure of the embryonic fissure (resulting in coloboma), retinal ganglion cells (optic-nerve hypoplasia/aplasia), and hyaloid vessels (persistent hyperplastic primary vitreous) cause disease (Brown and Tasman 1983). Most of these anomalies are sporadic, but autosomal dominant inheritance has been reported in families with coloboma of the optic nerve (CON [MIM 120430]) and optic-nerve hypoplasia (ONH [MIM 165550]). Mutations causing autosomal dominant syndrome have been identified in two transcription factor genes. The *PAX2* gene, one of nine known paired box genes, is expressed in the developing optic stalk, the ventral half of the optic cup, and the kidney, and its mutations cause papillorenal syndrome (PRS [MIM 120330]) (Sanyanusin et al. 1995). *HESX1* gene mutations, expressed in the ventral half of the forebrain, Ratke's pouch, and pituitary gland, were identified in patients with septo-optic dysplasia (SOD [MIM 182230]) (Dattani et al. 1998). However, there has not been genetic interpretation of various manifestations of optic-nerve malformations.

The *Pax6/PAX6* gene, first isolated as a candidate gene for human aniridia and expressed in developing CNS and various ocular tissues (Walther and Gruss 1991; Nishina et al. 1999), encodes a transcription factor that is involved in eye morphogenesis (Gehring 1996). Genetic analysis

Received December 30, 2002; accepted for publication March 24, 2003; electronically published April 29, 2003.

Address for correspondence and reprints: Dr. Noriyuki Azuma, Department of Ophthalmology, National Center for Child Health and Development, 2-10-1, Okura, Setagaya-ku, Tokyo 157-8535, Japan. E-mail: azuma-n@ncchd.go.jp

© 2003 by The American Society of Human Genetics. All rights reserved.
0002-9297/2003/7206-0021$15.00

has detected numerous *PAX6* mutations, not only in patients with aniridia but also with other eye anomalies (summarized in the Human *PAX6* Mutation Database). In situ hybridization and immunohistochemistry indicated *PAX6* expression in the developing optic nerve (Walther and Gruss 1991; Nishina et al. 1999), and the small eye (*Sey*^{H}) mouse mutant with a deletion of the *Pax6* locus showed coloboma, a defect of the initial invagination in the optic stalk and cup (Glaser et al. 1990). However, there is no evidence of *PAX6* mutations in patients with optic-nerve malformations.

We screened for *PAX6* mutations in genomic DNA from 155 individuals with a variety of congenital optic-nerve malformations by use of PCR-SSCP analysis. PCR primers used to amplify *PAX6* exons were synthesized on the basis of the reported sequence (Glaser et al. 1992); the primer sequences can be found in appendix A (online only), and the conditions of PCR and SSCP analyses were described elsewhere (Azuma et al. 1999). Nucleotide sequences were determined directly or after cloning into plasmid pUC18 by use of a Sequenase version 2 kit (Amersham) with PCR primers or universal primers in pUC18. Eight mutations were detected.

Patient 1, a 5-year-old girl, had bilateral morning glory disc anomaly. Mutation analysis identified 619C→T nucleotide substitution (according to GenBank accession number M93650), which is expected to result in P68S (fig. 1*a*). Patient 2, a 21-year-old male, had bilateral ONH and 1030C→T (Q205X) (fig. 1*b*). Patient 3, a 1-year-old boy, had an iris anomaly, large coloboma of the optic nerve, retina, and choroids, a remnant of hyaloid vessel proliferation (persistent hyperplastic primary vitreous) bilaterally, and growth and mental retardation; mutation analysis identified 1190T→C (F258S) (fig. 1*c*). Patient 4, a 2-year-old boy, had bilateral ONH, growth and mental retardation, an enlarged ventricle by computed tomography (CT) study, multiple spike and wave bursts by electroencephalogram, and vesicoureteral reflux; mutation analysis identified 1292G→T (S292I) (fig. 1*d*). Patient 5, a 1-year-old girl, had Peters anomaly in the left eye and slight corneal opacity, deep excavation of the optic-nerve head in the right eye, and 1504T→C (S363P) (fig. 1*e*). Patient 6, a 2-mo-old girl, had microphthalmos in the right eye, iris dysplasia and optic-nerve aplasia with a remnant of the hyaloid vessels in the left eye, and 1550A→G (Q378R) (fig. 1*f*). Patient 7, a 19-year-old male, had bilateral ONH and 1558A→G (M381V) (fig. 1*g*). Patient 8, a 4-mo-old girl, had bilateral optic-nerve aplasia and 1588A→G (T391A) (fig. 1*h*). Further clinical details can be found in appendix A (online only).

All patients except patients 3 and 4 had normal growth, intelligence, results of physical examination, and appearance on CT. Each had a normal karyotype. The mutations detected here occurred on one of the alleles (were thus heterozygous) and were not detected in unaffected immediate family members or in >100 normal individuals, indicating sporadic occurrence. Since mutations of the *PAX2* gene were detected in patients with optic-nerve anomalies associated with renal anomaly (PRS) (Sanyanusin et al. 1995), we screened for *PAX2* but failed to detect any mutation in these patients (data not shown).

Although all the mutations are indicated to be sporadic, each occurred in an important amino acid residue, which suggests that they cause disease. Seven of the eight mutations were missense, one of which was positioned in the paired domain (PD), one in the homeodomain (HD), and five in the proline-serine-threonine-rich transactivating domain (PST). The proline residue at 68 in the PD and the phenylalanine residue at 258 in the HD are conserved throughout all Pax family members identified to date. The serine residues at 292 and 363, the glutamine residue at 378, the methionine residue at 381, and the threonine residue at 391 in the PST are conserved throughout all the vertebrate Pax6 homologues identified to date. Amino acid sequences of the PST are conserved in vertebrates but considerably diversified in invertebrates.

We next performed functional assay of the mutations. The mutant forms of *PAX6* cDNAs, generated by PCR-based in vitro mutagenesis, were cloned into plasmids pBluescript and pCAGGS, the latter of which contains a cytomegalovirus enhancer and chicken β-actin promoter (Yamaguchi et al. 1997; Azuma et al. 1999). Wild-type and mutant forms of PAX6 proteins were synthesized by in vitro transcription and translation by use of rabbit reticulocyte lysate in the presence of [^{35}S] methionine. SDS-polyacrylamide gel electrophoresis and fluorography of the reactions revealed that the PAX6 proteins with expected molecular weights were produced at similar efficiency (data not shown). It is, therefore, unlikely that the mutations affect the efficiency of translation or stability of PAX6 protein.

To examine possible functional changes by the detected mutations, we performed a chloramphenicol acetyltransferase (CAT) assay in mouse embryonic carcinoma P19 cells, which are often used for functional analysis of the *PAX6* gene. First, a CAT-reporter construct carrying six copies of P6CON, the consensus binding sequence of the PAX6 PD (Epstein et al. 1994; Yamaguchi et al. 1997), was used. Wild-type PAX6 strongly activated CAT reporter-gene expression, and the transcriptional activation potential of PAX6 was more or less affected by all the mutations reproducibly, with significant impairment by P68S, Q205X, F258S, and S292I (fig. 2*b*). The mutation within the HD (F258S) impaired the PD-mediated transcriptional activation and is consistent with a report of the functional interplay of the PD and the HD (Mishra et al. 2002).

In the optic stalk and ventral forebrain of the zebrafish embryo, *Pax2* and *Pax6* expression is inversely correlated

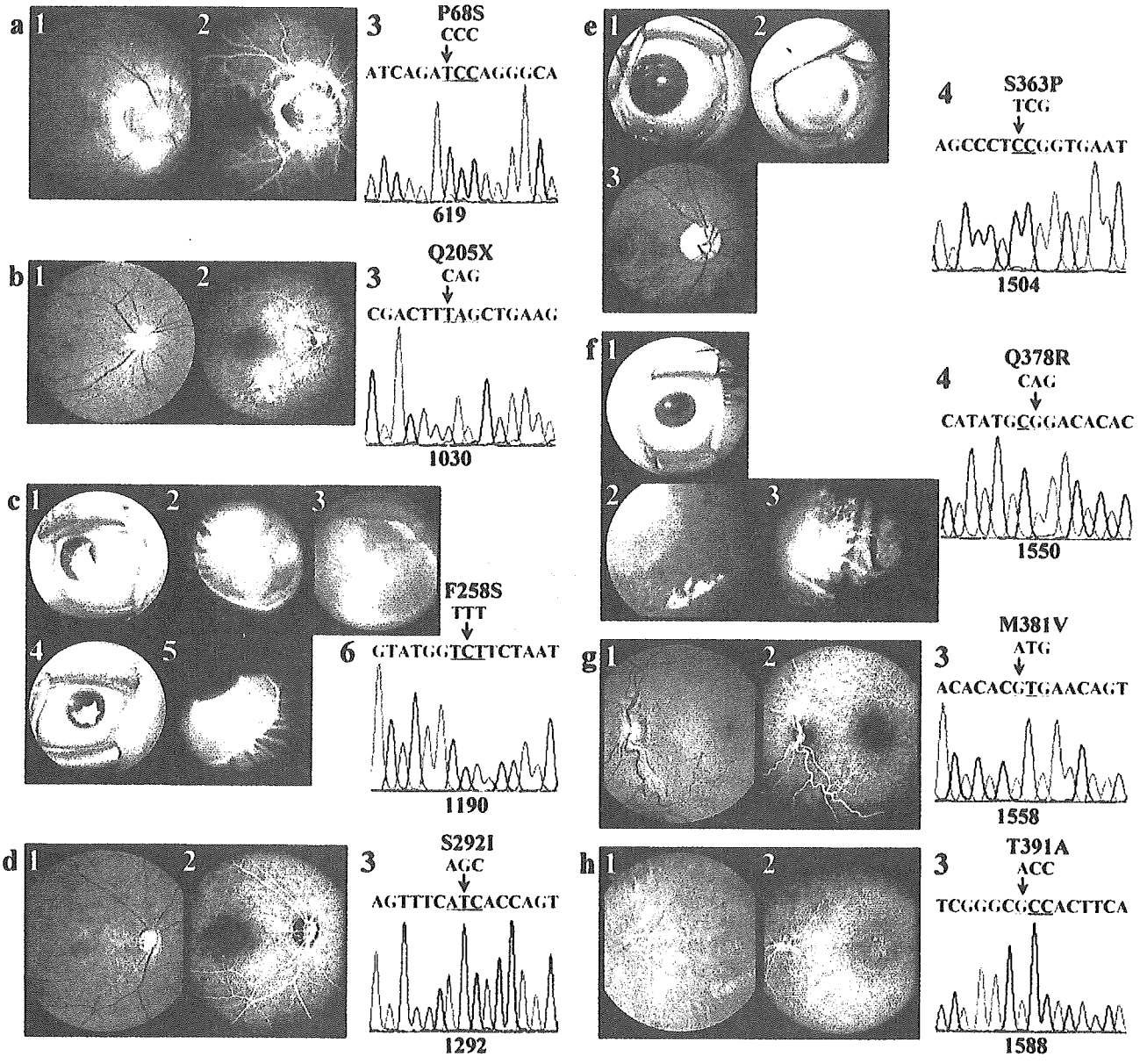

Figure 1 *a,* Fundus photography (*panel 1*) and fluorescein angiography (*panel 2*) of the right eye of patient 1, showing a morning glory disc anomaly. The optic-nerve region is excavated, and white tissue is present at the bottom. *Panel 3,* Mutation analysis identified 619C→T in exon 6 (P68S). *b,* Fundus photography (*panel 1*) and fluorescein angiography (*panel 2*) of the right eye of patient 2, showing a small optic-nerve head surrounded by a hypopigmented ring. *Panel 3,* Mutation detection of 1030C→T in exon 8 (Q205X). *c,* Photographs showing the anterior segments (*panel 1* and *panel 4*) and fundus (*panel 2, panel 3,* and *panel 5*) of patient 3. The iris was dysplastic and the posterior fundus showed large coloboma of the optic nerve, retina, and choroid. Hyaloid vessel proliferation is seen in the vitreous cavity. *Panel 6,* Mutation detection of 1190T→C in exon 10 (F258S). *d,* Fundus photography (*panel 1*) and fluorescein angiography (*panel 2*) of the right eye of patient 4, showing ONH. *Panel 3,* Mutation detection of 1292G→T in exon 10 (S292I). *e,* The right eye of patient 5 has a slight corneal opacity and iridocorneal adhesion (*panel 1*) and deep excavation of the optic-nerve head (*3*). The left eye has substantial corneal opacity (*panel 2*). *Panel 4,* Mutation detection of 1504T→C in exon 12 (S363P). *f,* The anterior segment (*panel 1*), fundus photography (*panel 2*), and fluorescein angiography (*panel 3*) of the left eye, with optic-nerve aplasia, of patient 6. The iris was dysplastic, and the optic-nerve head and retinal vessels were absent, with a remnant of the hyaloid vessels. *Panel 4,* Mutation detection of 1550A→G in exon 12 (Q378R). *g,* Fundus photography (*panel 1*) and fluorescein angiography (*panel 2*) of the left eye, with ONH, of patient 7. *Panel 3,* Mutation analysis identified 1558A→G in exon 12 (M381V). *h,* Fundus photography (*panel 1*) and fluorescein angiography (*2*) of the left eye, with optic-nerve aplasia, of patient 8. *c,* Mutation analysis identified 1588A→G in exon 12 (T391A).

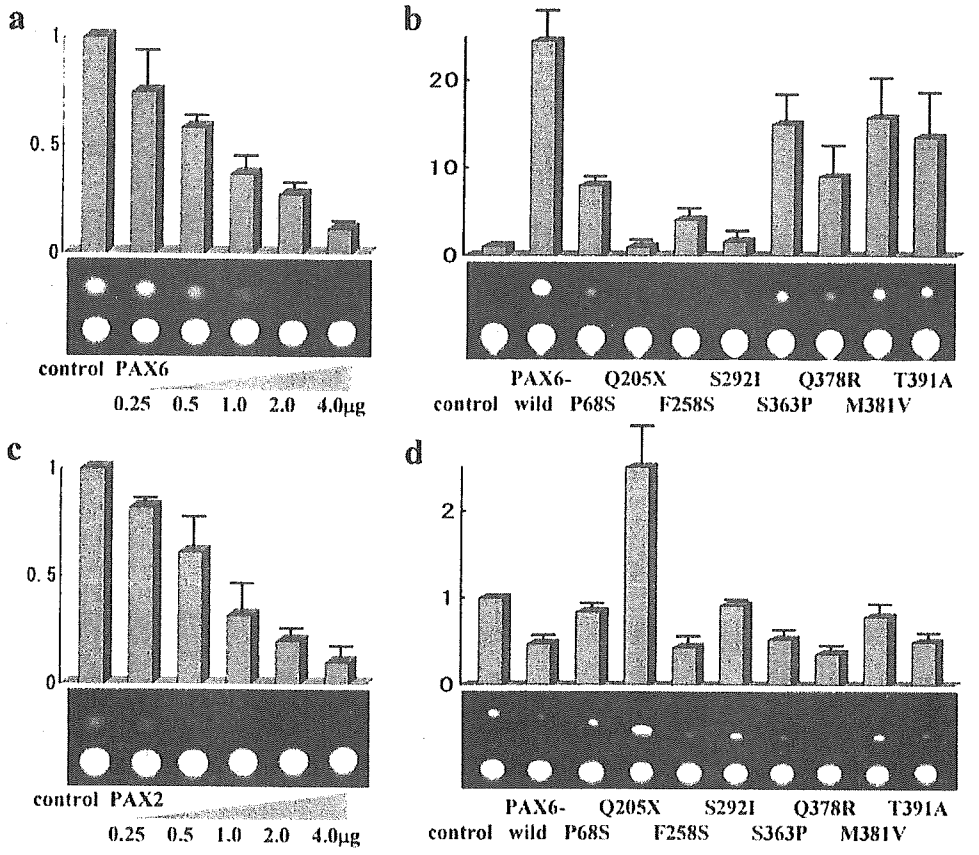

Figure 2 Effects of PAX6 on *PAX2* (*a*) and of PAX2 on *PAX6* (*c*). CAT activities were measured in P19 cells after cotransfection of effecter and reporter constructs. Total volume of DNA was adjusted with an empty vector, pBluescript. Cell extracts were prepared after 48 h and assayed for CAT activities by use of a FAST CAT Green Reagent (Molecular Probes). The CAT activity was quantified by measurement with a phospho-fluor-imager (Molecular Dynamics) and illustrated in a fold-activation, compared with the condition with the vector alone. The levels of *PAX2* were suppressed with increasing amounts of wild type of PAX6, and vice versa. *b*, Transactivating potential of PAX6 mutants. 0.1 μg of effecter construct and 1 μg of reporter constructs were cotransfected in P19 cells. Transcription level from P6CON was disturbed significantly by P68S, Q205X, F258S, and S292I mutants and slightly by S363P, Q378R, M381V, and T391A mutants. *d*, Effects of PAX6 mutants on *PAX2* expression. One μg of effecter construct and 1 μg of reporter constructs were cotransfected in P19 cells. The decreasing level of PAX6 was significantly disturbed with the P68S, Q205X, S292I, and M381V mutants. Each photograph of CAT assay under the bar graph is representative of at least three independent experiments.

under the control of sonic hedgehog signaling (Macdonald et al. 1995). Data indicating reciprocal transcriptional repression of *Pax2* and *Pax6* also were obtained using mouse homologues (Schwarz et al. 2000). Thus, although PAX2 and PAX6 were initially considered to be transcriptional activators, they also may inhibit transcription of some genes to exert their roles during development. We next examined the effect of PAX6 and PAX2 proteins on activities of *PAX2* and *PAX6* gene promoters, respectively. A CAT-reporter construct carrying an ~2-kb *PAX6* promoter region (the 1285th to 3381st nucleotides in GenBank accession number U63833), or a 1.2-kb *PAX2* promoter region (the −1002nd to +190th nucleotides in GenBank accession number U45245) was used. When an increasing amount of the *PAX6* or *PAX2* expression construct was cotransfected into P19 cells with a constant amount of the *PAX2* or *PAX6* reporter construct, each CAT activity decreased in a dose-dependent manner, indicating that PAX6 represses *PAX2* gene expression and vice versa (fig. 2*a* and 2*c*). By use of this assay system, we evaluated possible effects of the PAX6 mutations on *PAX2* promoter activity. Four expression constructs carrying P68S, Q205X, S292I, or M381V mutations failed to repress the *PAX2* promoter activity, unlike the wild-type PAX6 and other mutant constructs (fig. 2*d*). These mutations were found with morning glory disc anomaly or ONH and caused a functional change in our experimental system. Because *PAX2* mutations were also found in coloboma and ONH (Sanyanusin et al. 1995), we speculate that failure of the PAX6-PAX2 regulatory circuit may affect phenotypic manifestations of these anomalies. Ex-

pression of the CAT-reporter gene was probably inhibited by endogenous PAX6 protein to some extent and stimulated by Q205X through its dominant-negative action on endogenous *PAX6*, as suggested elsewhere (Singh et al. 1998). Numerous processes are needed for optic-nerve formation, so *PAX2* and *PAX6* may cooperate in optic-nerve formation or occasionally share tasks; for example, opening and closing the embryonic fissure and mutations of either gene cause similar phenotypic changes.

Our patients had a wide variety of optic-nerve malformations, in which a full series of disease-causing events of optic-nerve malformation—including embryonic fissure (coloboma), retinal ganglion cells (ONH/aplasia), and hyaloid vessels (persistent hyperplastic primary vitreous)—are included (Brown and Tasman 1983). Because *Pax6/PAX6* is expressed in numerous tissues important for optic-nerve development—including the CNS, optic stalk, and retinal progenitors at an early stage, and retinal ganglion cells at a late stage—it is not surprising that many more variable phenotypes are caused by *PAX6* mutations than by *PAX2* mutations.

Genetic analysis indicated that haploinsufficiency of the gene causes the classical aniridia phenotype, in which all eye tissues are affected. Most mutations detected in aniridia result in premature translational termination on one of the alleles (Martha et al. 1994). In contrast, most missense mutations generate distinctive nonaniridia phenotypes—including anterior segment anomalies, congenital cataracts, and foveal hypoplasia—in which certain eye tissue is affected (Hanson et al. 1999). Because most of the amino acid residues are conserved, distinct missense mutations may alter the degree and specificity of DNA binding and transcriptional regulation by PAX6 protein to a different extent (Yamaguchi et al. 1997; Azuma et al. 1999). Some missense mutations are thought to be recurrently associated with a specific phenotype in eye anomalies. Two patients with an R128C mutation, independently identified in Japan and Europe, had the same phenotype, with foveal hypoplasia (Azuma et al. 1996; Hanson et al. 1999). Mutations associated with Peters anomaly were in the N-terminal subdomain of the PD (van Heyningen and Williamson 2002). In contrast, a missense mutation in the alternatively spliced exon was associated with a variety of ocular anomaly phenotypes (Azuma et al. 1999). No distinct positional effect of the missense mutations on phenotypic manifestation of optic-nerve malformations was found in the present study. Because the *Pax6/PAX6* gene is expressed repeatedly throughout ocular tissues, these missense mutations probably disturb PAX6 protein function in different ways, which result in various phenotypes.

Besides eye anomalies, patient 3 was mentally retarded, and patient 4 had an enlarged CNS ventricle and a urinary anomaly. *PAX6* plays an important role in CNS development, and CNS malformation and mental retardation associated with *PAX6* mutations have been reported (Malandrini et al. 2001; Sisodiya et al. 2001). However, gene expression in the urinary tract was not reported. It is unknown if patient 4 carries compound mutations of the separate genes related to eye or urinary-tract development, or whether *PAX6* is slightly, or for a short time, expressed in the urinary tract. Because *PAX2* is expressed in the kidney, extensive analysis of expression and correlation of *PAX6* and *PAX2* throughout development would validate the significance of the genes in pathogenesis of the diseases in which multiple organs are involved.

Acknowledgment

This study was supported by grants for genome, tissue engineering biotechnology; for sensory and communicative disorders; and for pediatric research from the Ministry of Health, Labor, and Welfare, Japan; and by a grant for organized research combination system from the Ministry of Education, Culture, Sports, Science, and Technology, Japan.

Electronic-Database Information

Accession numbers and URLs for data presented herein are as follows:

GenBank, http://www.ncbi.nlm.nih.gov/Genbank/ (for human *PAX6* mRNA [accession number M93650], human *PAX6*, promoter and exons 1 and 2 [accession number U63833], human *PAX2*, promoter and exon 1 [accession number U45245])

Human *PAX6* Mutation Database, http://pax6.hgu.mrc.ac.uk/Tables/tables.htm

Online Mendelian Inheritance in Man (OMIM), http://www.ncbi.nlm.nih.gov/Omim/ (for CON, ONH, PRS, and SOD)

References

Azuma N, Nishina S, Yanagisawa H, Okuyama T, Yamada M (1996) PAX6 missense mutation in isolated foveal hypoplasia. Nat Genet 13:141–142

Azuma N, Yamaguchi Y, Handa H, Hayakawa M, Kanai A, Yamada M (1999) Missense mutation in the alternative splice region of the PAX6 gene in eye anomalies. Am J Hum Genet 65:656–663

Brown GC, Tasman WS (1983) Congenital anomalies of the optic disc. Grune & Stratton, New York

Dattani MT, Martinez-Barbera JP, Thomas PQ, Brickman JM, Gupta R, Martensson IL, Toresson H, Fox M, Wales JK, Hindmarsh PC, Krauss S, Beddington RS, Robinson IC (1998) Mutations in the homeobox gene *HESX1/Hesx1* associated with sepro-optic dysplasia in human and mouse. Nat Genet 19:125–133

Epstein JA, Cai J, Glaser T, Jepeal L, Maas RL (1994) Identification of a Pax paired domain recognition sequence and

evidence for DNA-dependent conformational changes. J Biol Chem 269:8355–8361

Gehring WJ (1996) The master control gene for morphogenesis and evolution of the eye. Genes Cells 1:11–15

Glaser T, Lane J, Housman D (1990) A mouse model of the aniridia-Wilmus tumor deletion syndrome. Science 250:823–827

Glaser T, Walton DS, Maas RL (1992) Genomic structure, evolutionary conservation and aniridia mutation in the human PAX6 gene. Nat Genet 1:232–239

Hanson I, Churchill A, Love J, Axton R, Moore T, Clarke M, Meire F, van Heyningen V (1999) Missense mutations in the most ancient residues of the PAX6 paired domain underlie a spectrum of human congenital eye malformations. Hum Mol Genet 8:165–172

Macdonald R, Barth KA, Xu Q, Holder N, Mikkola I, Wilson SW (1995) Midline signalling is required for Pax gene regulation and patterning of the eyes. Development 121:3267–3278

Malandrini A, Mari F, Palmeri S, Ganbelli S, Berti G, Bruttini M, Bardelli AM, Williamson K, van Heyningen V, Renieri A (2001) PAX6 mutation in a family with aniridia, congenital ptosis, and mental retardation. Clin Genet 60:151–154

Martha A, Ferrell RE, Mintz-Hittner H, Lyons LA, Saunders GF (1994) Paired box mutations in familial and sporadic aniridia predicts truncated aniridia proteins. Am J Hum Genet 54:801–811

Mishra R, Gorlov IP, Chao LY, Singh S, Saunders GF (2002) PAX6, paired domain influences sequence recognition by the homeodomain. J Biol Chem 277:49488–49494

Nishina S, Kohsaka S, Yamaguchi Y, Handa H, Kawakami A, Fujisawa H, Azuma N (1999) PAX6 expression in the developing human eye. Br J Ophthalmol 83:723–727

Sanyanusin P, Schimmenti LA, McNoe LA, Ward TA, Pierpont ME, Sullivan MJ, Dobyns WB, Eccles MR (1995) Mutation of the *PAX2* gene in a family with optic nerve colobomas, renal anomalies and vesicoureteral reflux. Nat Genet 9:358–364

Schwarz M, Cecconi F, Bernier G, Andrejewski N, Kammandel B, Wagner M, Gruss P (2000) Spatial specification of mammalian eye territories by reciprocal transcriptional repression of Pax2 and Pax6. Development 127:4325–4334

Singh S, Tang HK, Lee JY, Saunders GF (1998) Truncation mutations in the transactivation region of PAX6 results in dominant-negative mutants. J Biol Chem 273:21531–21541

Sisodiya SM, Free SL, Williamson KA, Mitchell TN, Willis C, Stevens JM, Kendall BE, Shorvon SD, Hanson IM, Moore AT, van Heyningen V (2001) *PAX6* haploinsufficiency causes cerebral malformation and olfactory dysfunction in humans. Nat Genet 28:214–216

van Heyningen V, Williamson KA (2002) *PAX6* in sensory development. Hum Mol Genet 11:1161–1167

Walther C, Gruss P (1991) Pax-6, a murine paired box gene, is expressed in the developing CNS. Development 113:1435–1449

Yamaguchi Y, Sawada J, Yamada M, Handa H, Azuma N (1997) Autoregulation of Pax6 transcriptional activation by two distinct DNA-binding subdomains of the paired domain. Genes Cells 2:255–261